

# EVALUATION OF MULTIAXIAL TEST DATA OF UD-LAMINAE BY SO-CALLED "FRACTURE-TYPE STRENGTH CRITERIA" AND BY SUPPORTING PROBABILISTIC MEANS

*Ralf G. Cuntze*

*Division of Spacecraft, MAN Technologie AG  
Liebigstr. 5a, 85757 Karlsfeld/Munich. Fax 0049-8131-89-1939  
(lecturer at Universität der Bundeswehr, München)*

## SUMMARY

Overall objective of this elaboration is to calibrate fracture criteria resp. to define size and shape of the fracture body as cheaply as possible by executing the characteristic tests only.

Based on knowledge, achieved by investigating *v. Mises*, *Mohr - Coulomb* and the new physically based *Hashin - Puck* Strength Criteria for inter fibre fracture (IFF) of brittle unidirectional laminae, a new and general concept for the derivation of fracture criteria will be proposed and applied to fibre reinforced plastics (FRP).

The fracture body derived here is basically piecewise smooth, each piece representing a single *failure mode*. As interpolation functions the *invariants* associated to the material's symmetries are utilised. Physical basis is the reference to the 2 fracture-types in a material: normal fracture (NF) and shear fracture (SF). For the subsets of failure modes "fibre fracture (FF)" and "IFF" two conditions for FF and three for IFF are derived. These five conditions describe the five failure modes or mechanisms occurring, and five failure modes are the maximum number a transversally-isotropic material, modelled a crystal, can possess.

In the transition zone of two failure modes or domains of mixed fracture, respectively, a probabilistic modelling has to be applied. This finally leads again to a smooth surface of the complete fracture body.

As the most remarkable results of the elaboration have to be pointed out: Consider micromechanics resp. real material stresses in the constituents fibre and matrix (incl. interface) which only can fail, however, formulate and visualise in lamina stresses at composite resp. macromechanical level and think in Mohr's fracture stresses.

The application of the criteria to test results is very promising. Erroneous results, possible if applying the traditional global (stress) interaction criteria, should not be achieved.

**Keywords:** Fibre reinforced composites, strength criteria, test data evaluation

## 1 INTRODUCTION

"Hot spots" of load carrying isotropic structures have to be designed versus various (Fig. 1) strength failure modes including *onset of yielding* and *fracture* resp. *onset of cracking*.

In case of laminates built from brittle UD-laminae the stress man has to dimension each lamina (ply-by-ply) versus IFF and fibre-fracture (FF). Whereas IFF indicates the onset of *fibre-parallel cracking* in one lamina of the laminate FF will indicate the onset of *fibre cracking*. First FF of a lamina usually marks the final fracture of the laminate. A reliable prediction of IFF under 3D-states of stress is mandatory for the calculation of progressive failure.

As well in the stress analysis as in the failure criterion of the strength analysis there are scattering design parameters. The uncertainty of these parameters (loads, strengths, geometrical quantities, young's module, ...) is of *physical nature* or of *statistical nature* (shortage of information due to a too small sample size of a certain design parameter

measured). Besides this there is always some *uncertainty in the calculation model*. This scatter is usually considered in the design by the use of fixed, deterministic *factors of safety*, better called *design factors of safety* (DFOS), which are based on experience with structural tests. In aerospace industry structures are dimensioned by using DFOS  $j$  which increase the so-called *design limit load* (DLL) to the design ultimate load (DUL) according to  $j_{ult} \cdot DLL$ . This procedure includes the idea of *proportional loading* and that the reserve factor  $f_{Res}$  is related to the external load only. Above "load factors" are discriminating the *onset of yield* (e.g.  $j_{po,2} = 1.1$ ) for isotropic material and *ultimate fracture* (e.g.  $j_{ult} = 1.5$ ). The design allowables to be used as strength values are statistics-based minimum values [Cun96/2]. This might be a so-called Mil-Hdbk 17 "B-value" with 90 % reliability and 95 % confidence probability, the latter number regards the confidence in the transfer of the finite number of sample test data to the parent distribution with its infinite number of data.

*Proofs of Design* or *design verifications* done by analysing and/or testing a structure have to be given for *failure modes* such as stability, deformation, vibration and strength. Target of the designer is to achieve a margin of safety  $MS \geq 0$  for each single failure mode and - in this paper - for fracture modes as a subset of them. In order to achieve a reliable margin of safety ( $MS = f_{Res} - 1$ ) in the Strength Proof of Design the engineer should accurately know the normally non-linear 3D-state of stress in the critical material element and its separation into load-induced and residual stresses!

*Fracture* criteria as a subset of *strength* criteria should enable the engineer to perform the Strength Proof of Design for any 3-dimensional state of stress resp. combination of stresses with a *minimum* amount of test data.

*Verified* fracture criteria as a subset of strength criteria (Fig. 1) enable to do this. They can be calibrated after execution of the *basic strength* tests, only.

The traditional criteria such as Tsai/Wu have some shortcomings which forces research to correct or replace them [VDI97]. However, in the last four years heavy progress has been made in Germany with the derivation of more physically-based fracture criteria for brittle unidirectional isolated laminae. On the basis of [Has80] A. Puck developed the "Hashin-Puck (Action-Plane) Strength Criteria" for IFF [Puc92] assuming 2 modes. Additionally, tests were performed under a German grant to verify the criteria [VDI97].

Parallel, the author tried to generate strength criteria, each of which should be related to one single failure mechanism resp. fracture *mode* (not *type*) and formulated by *invariants*, thus taking the material's symmetries into account. Basis are the *types of fracture in a material* which are normal stress induced fracture (NF) and shear stress induced fracture (SF). This

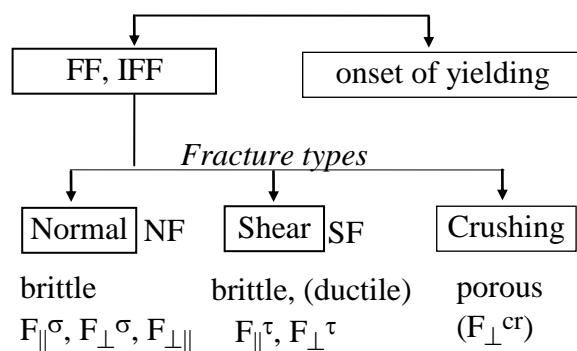


Fig. 1:  
Strength Failure Modes (modi) of Composites.  
(NF = normal fracture, SF = shear fracture.  
 $F_{||}^{\sigma}, \dots, F_{\perp}^{cr}$  are the UD-lamina's failure  
functions representing fracture modes)

fracture-type concept proposed may be applied to *any* brittle or ductile behaving material [Cun96/2].

In this paper brittle UD-laminae are described, only. The fracture criteria derived are *stress* criteria and have as foundations: The material is *homogeneous* (smeared or averaged material)

and can be modelled an *ideal crystal* with its symmetries and mutual independent basic strengths from a meso/macromechanical point of view. However, for the in reality heterogeneous composite (is a structure not a material) the micromechanical behaviour of the constituents (real materials) fibre, matrix and interphase will be considered too.

## 2 FRACTURE MECHANISMS IN UD-LAMINAE

Fracture is understood in this article as a separation of material, which is free of damage such as cracks but not free of defects and flaws prior to loading. In this context *crushing* of a porous material has to be seen a separate *fracture mechanism* resp. (*fracture*) *failure mode* and *type*.

Idealising a material a crystal one can draw from Table 1 the information: The number of symmetries determines the number of strengths. The higher the *structural level* of the material the more basic strengths have to be measured. Due to the fact 5 strengths being usually measured in case of a transversally-isotropic lamina the application of the crystal model is still general practice.

Table 1 : Number of Strengths and Fracture Types for Various Ideal Materials ( $t = tension$ ,  $c = compression$ ;  $\parallel, \perp = parallel, transversal$  to the fibre;  $W = warp$ ,  $F = fill$ . Superscript  $c = critical$ )

material has	no structure	increasing structural level $\rightarrow$	
	0	1	2
allocation to crystal type	isotropic	transversally isotropic	rombically anisotropic
symmetries	2	5	9
material example	resin matrix, mono. ceramics	UD-lamina, mat	fabrics
elasticity quantities	$E, \nu$ (2)	$E_{\parallel}, E_{\perp}, G_{\parallel\perp}$ $\nu_{\perp\parallel}, \nu_{\perp\perp}$ (5)	$E_W, E_F, G_{WF}, \nu_{FW}, E_3,$ $\nu_{3W}, \nu_{3F}, G_{F3}, G_{W3}$
strength quantities ( <i>resistances</i> )	$R^t, R^c$ or ( $R_{\sigma}, R_{\tau}$ ) (2)	$R_{\parallel}^t, R_{\parallel}^c, R_{\perp}^t,$ $R_{\perp}^c, R_{\perp\parallel}$ (5)	$R_W^t, R_W^c, R_F^t, R_F^c, R_3^t,$ $R_{3W}, R_{FW}, R_{3F}, R_3^c$ (9)
invariants	$I_1, I_2,$ or $J_2 \dots$	$I_1, \dots, I_5, \dots$	$I_1, \dots, I_7, \dots$
fracture toughnesses	$K_{Ic}^t, K_{IIc}^c$ (2)	$K_{\parallel c}^t, K_{\parallel c}^c, K_{\perp c}^t$ $K_{\perp c}^c, K_{\perp\parallel c}$ (5)	

Fig. 2 shall give answer to the question: How many *types of fracture* are recognised in case of isotropic and transversally-isotropic *ideal materials*? These are just two: the shear stress induced fracture SF (Mohr's stress  $\tau_n$  is acting at the "plane" of fracture) and normal stress  $\sigma_n$  induced fracture NF - as we know - for isotropic materials, but also two for the UD-material. However, the latter case comprises several SF and NF which belong to FF and IFF.

Also the physical fracture "planes" are pointed out in the figure.

A comparison of Fig. 2 with Table 1 leads to an essential conclusion: *One strength governs one distinct fracture type*.

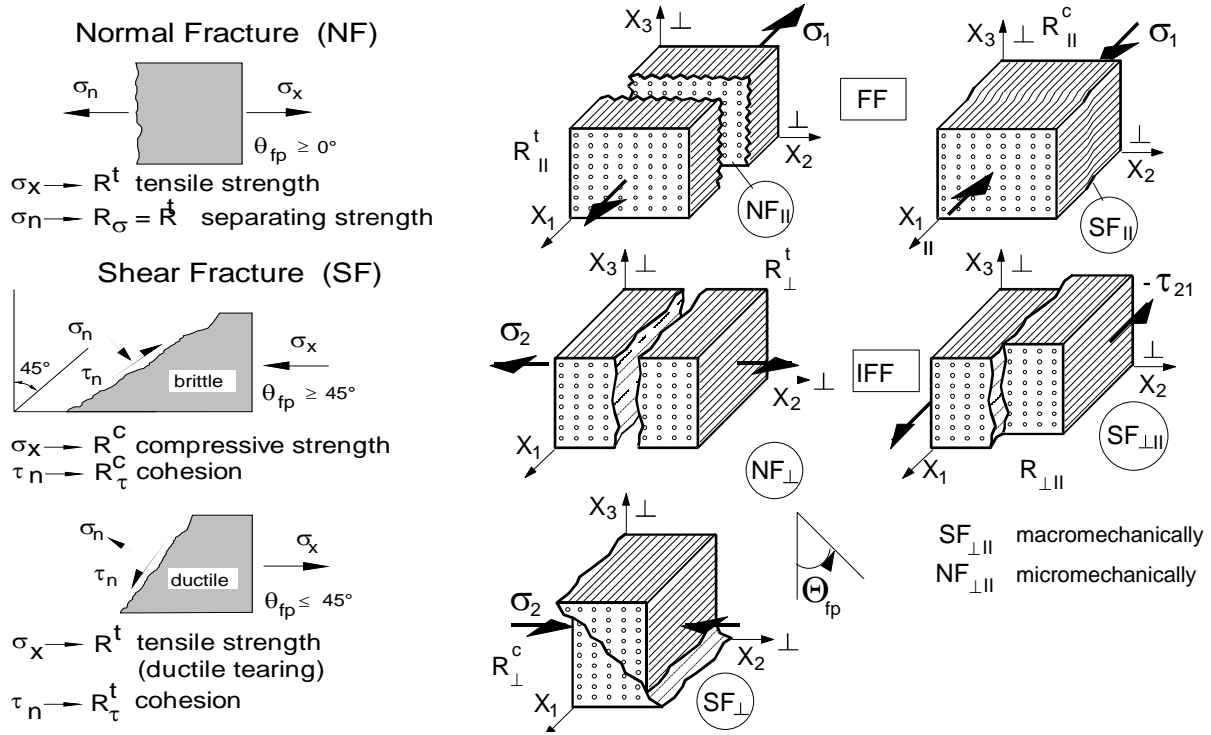


Fig. 2: Fracture Types ( $\equiv$  modes) in case of Brittle and Ductile behaving Isotropic Material and Fracture Modes in case of Transversally-isotropic Material ( $\sigma_n^A (\theta = \theta_{fp}) = \sigma_n$ ).

The characterisation of the strength of transversally-isotropic composites requires the measurement of five independent basic strengths:  $R_{||}^t$ ,  $R_{||}^c$  (fibre parallel tensile and compressive strength) as well  $R_{\perp}^t$ ,  $R_{\perp}^c$  (tensile, compressive strength perpendicular to the fibre direction) and  $R_{\perp||}$  (fibre parallel shear strength).  $R_{||}^t$  is determined by the strength of the constituent fibre,  $R_{||}^c$  is generally governed by *shear stability*. This includes different microfailure mechanisms: The matrix may shear under loading and does not stabilise the generally somewhat misaligned fibres embedded. Hence it comes to bending and "kinking" (structure behaviour). But, the load "grasping" fibre as the well-stabilised, stiffer constituent may shear (this is material behaviour) under  $\sigma_{||}^c$  and  $\tau_{\perp||}$ , too.  $R_{\perp}^t$  is determined as well by the relatively low strength properties of the matrix (cohesive failure) and the interphase material in the interface fibre-matrix (adhesive failure caused by a weak fibre-matrix bond), as by the fibres acting as embedded stress risers.

Well known from literature is the shift of the fracture limit of IFF strain resp. stress to higher values the absolutely thinner the lamina is and the stiffer in comparison the embedding laminae and the laminate are. Whereas the free isolated lamina (UD-specimen) if transversally tensile loaded is underlying a weakest-link failure (resulting in a Weibull distribution for  $R_{\perp}^t$ ) the embedded lamina will be strain controlled by its neighbours. Inherent defects or microcracks as often reported can grow together to form mesocracks *only* in case they have a chance to open. However, these microcracks are arrested fracture-mechanically by the embedding laminae.

In order to consider the constraint effect on a "thin" embedded lamina following [Fla 82] and some own investigations the author recommends e.g. for CFRP ( $t_{thr} \approx 0,35$  mm) as correction formula for the design allowable  $R_{\perp}^t$  due to

$$R_{\perp}^t (t_{\perp} < t_{thr}) = R_{\perp}^t \sqrt{t_{thr} / t_{\perp}} . \quad (2.1)$$

### 3 GENERAL FORMULATIONS OF STRENGTH CRITERIA AND CONDITIONS

Strength criteria  $F \stackrel{>}{\underset{<}{=}} 1$  are generally formulated as (isotropic case shown for simplicity)

$$F(\{\sigma\}; \{R\}) = F(\sigma_x, \sigma_y, \sigma_z, \tau_{zy}, \tau_{zx}, \tau_{yx}; R^t, R^c) \stackrel{>}{\underset{<}{=}} 1 \quad \dots \text{ criterion.} \quad (3.1)$$

In the failure (here fracture) function  $F$  the vector  $\{\sigma\}$  contains the six stresses in the coordinate system of the structure - as above - or the six lamina stresses. The vector  $\{R\}$  contains all *basic strengths* to be applied such as  $R^t, R^c$  in isotropic case.

Failure surfaces are determined by the strength condition  $F = 1$

$$F(f_{Res} \{\sigma\}; \{R\}) = 1 \quad \dots \text{ condition} \quad (3.2)$$

To achieve this, the stresses in equation 3.1 have to be multiplied by the reserve factor  $f_{Res}$ , which is usually dropped for reasons of a simpler writing.

Composites with a polymeric matrix exhibit brittle behaviour from a macroscopic point of view. Thus a formulation of strength criteria can be based on the fracture hypotheses of *Mohr* and *Coulomb*, adapted to UD-laminae. This was suggested by Hashin [Has80]. Hence, using Mohr's fracture stresses, which act together at the *same plane*, the isotropic equations read:

$$\begin{aligned} F_\sigma &= F(\{\sigma^{Mohr}\}, R_\sigma) = 1 \quad \dots \dots \dots \text{NF} & (3.3a) \\ &= \sigma_n / R_\sigma = 1 \quad \quad \quad (\text{normal stress hypothesis}) \end{aligned}$$

$$\begin{aligned} F_\tau &= F(\{\sigma^{Mohr}\}, R_\tau) = 1 \quad \dots \quad \dots \dots \text{SF} & (3.3b) \\ &= \tau_n / (R_\tau - \mu \sigma_n) = 1 \quad \text{e.g. (shear stress hypothesis, Mohr-Coulomb)} \end{aligned}$$

with  $R_\sigma$ : = separating strength (resistance)  $R_\tau$ : = cohesion (resist.),  $\mu$ : = Coulomb friction.

This outlines: *one* condition is to be used for *each* fracture mechanism which is dominated by *one fracture resistance*  $R_\sigma$  or  $R_\tau$  (s. also [Cun96/2] for isotropic materials). A resistance (of the fracture plane) corresponds with the basic strength associated if the action plane of a distinct stress comes to be the potential (load must be high enough, too) fracture plane: e.g. in brittle case  $\max \sigma = R_\sigma = R^t$  (isotropic) or  $R_\perp^t$  (transversally-isotropic). In case of brittle behaviour only  $R_\sigma$  can be measured and vice versa  $R_\tau$  in case of ductile behaviour. Therefore,  $R_\tau$  principally remains undeterminable until the fracture angle  $\theta_{fp}$  is determined. This is also valid for the *fracture plane stresses*  $\{\sigma^{Mohr}\}$ .

The "curve fitting" of the course of test data can be performed much easier by not taking Mohr's stresses and the 2 resistances  $R_\sigma, R_\tau$  but  $\{\sigma\}$  and the 2 basic strengths. However, equation (3.1) will now be used in Mohr's sense meaning one basic strength governs one fracture mechanism NF or SF

$$F_\sigma = F(\{\sigma\}, R^{NF}) = F(\{\sigma\}, R^t) = 1 \quad \text{and} \quad F_\tau = F(\{\sigma\}, R^{SF}) = 1. \quad (3.4)$$

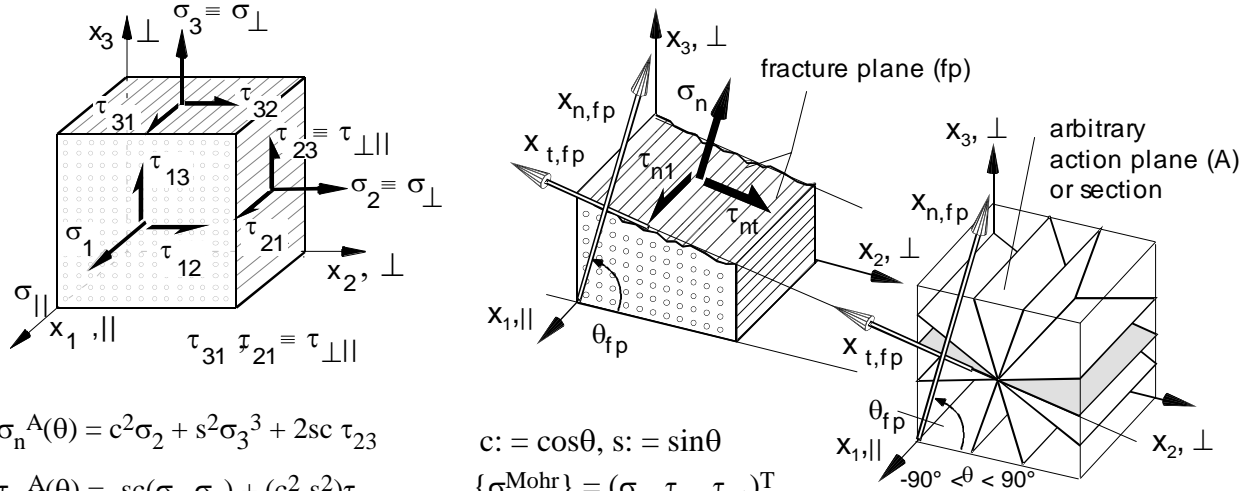
Both, the physical basis and the numeral handling are improved by using invariants as interpolation functions, a well known and classical approach.

### 4 DERIVATION OF "FRACTURE-TYPE STRENGTH CRITERIA"

#### 4.1 Description of 3D-States of Stress

Three-dimensional states of stress in a lamina may be described by lamina stresses  $\{\sigma\}$ . A further possibility is given by using *Mohr's fracture stresses* mentioned above. They are acting in the potentially physical fracture "plane" (Fig. 3) and are decisive for fracture. In case of

normal (stress induced) fracture  $\sigma_n$  will be responsible for fracture and in case of shear (stress induced) fracture  $\tau_n$  will be the fracture dominating one. Fig. 3 does also explain how



$$\begin{aligned}\sigma_n^A(\theta) &= c^2\sigma_2 + s^2\sigma_3 + 2sc\tau_{23} \\ \tau_{nt}^A(\theta) &= -sc(\sigma_2 - \sigma_3) + (c^2 - s^2)\tau_{23} \\ \tau_{nl}^A(\theta) &= c\tau_{21} + s\tau_{31}\end{aligned}$$

$$\begin{aligned}c &= \cos\theta, s = \sin\theta \\ \{\sigma^{\text{Mohr}}\} &= (\sigma_n, \tau_{nt}, \tau_{nl})^T\end{aligned}$$

Fig. 3: 3D-states of Stress (lamina stresses and Mohr's stresses at the fracture plane)

Mohr's fracture stresses are derived by transformation of  $\{\sigma\}$  into a fibre-parallel plane  $\{\sigma(\theta)\} = [T(\theta)]\{\sigma\}$ , ([Cun94]). Fracture plane will become that plane where the effort E under  $\{\sigma(\theta)\}$  will be the maximum or  $f_{\text{Res}}$  will become a minimum, if  $\sigma_n = \sigma_n^A(\theta_{\text{fp}})$  etc.

A comprehensive way to describe states of stress is given if using invariants formed by the lamina stresses (s. [Has80], [Boe85]). Table 2 depicts the invariants for a transversally-isotropic UD-lamina ( $I_3 = \text{square of max } \tau_{\perp\parallel}, I_4 \approx \text{square of max } \tau_{\perp\perp}$ ):

$$\begin{aligned}I_{1f} &= v_f \sigma_{1f} & \text{Table 2: Invariants of a UD-lamina} \\ I_2 &= \sigma_2 + \sigma_3 = \sigma_n + \sigma_t = \sigma_{\parallel} + \sigma_{\text{III}} & (v_f = \text{fibre volume fraction; index } f \text{ for fibre}) \\ I_3 &= \tau_{31}^2 + \tau_{21}^2 = \tau_{t\parallel}^2 + \tau_{n\perp}^2, & I_5 = (\sigma_2 - \sigma_3)(\tau_{31}^2 - \tau_{21}^2) + 4\tau_{23}\tau_{31}\tau_{21}. \\ I_4 &= (\sigma_2 - \sigma_3)^2 + 4\tau_{23}^2 = (\sigma_n - \sigma_t)^2 + 4\tau_{nt}^2 & \text{or } I_4 = \tau_{23}^2 - \sigma_2\sigma_3 = -\sigma_{\parallel}\sigma_{\text{III}}.\end{aligned}$$

## 4.2 Fracture-type strength conditions

Table 3 summarises the author's proposal for fracture-type strength conditions being applied later to glass fibre reinforced plastics (GFRP).

Table 3: Fracture-type Strength Conditions for Transversally-isotropic Laminae. ( $f_{\text{Res}}$  dropped in the equations; characteristic basic strength depicted;  $\tau$  and  $\sigma$  indicate the responsible stress. The correction terms for IFF considering  $\sigma_f$  are not depicted here, see [Cun96/1])

- Fibre Fracture (FF) -

$$F_{\parallel}^{\sigma}: a_{\parallel}^{\sigma} \cdot I_{1f} = R_{\parallel}^t \quad \text{and} \quad F_{\parallel}^{\tau}: a_{\parallel}^{\tau} \cdot I_{1f} + b_{\parallel}^{\tau} I_3 = R_{\parallel}^c \quad \dots \text{NF}_{\parallel} \text{ and SF}_{\parallel}$$

- Inter Fibre Fracture (IFF) - (matrix, interface) -

$$F_{\perp}^{\sigma}: a_{\perp}^{\sigma} I_2 + b_{\perp}^{\sigma} \sqrt{I_4} + c_{\perp}^{\sigma} I_2^2 / R_{\perp}^t + [d_{\perp}^{\sigma} I_3 + (e_{\perp}^{\sigma} I_2 I_3 + f_{\perp}^{\sigma} I_5) R_{\perp}^t / R_{\perp\parallel}] / R_{\perp\parallel}^2 = R_{\perp}^t \quad \dots \text{NF}_{\perp}$$

$$F_{\perp\parallel}: a_{\perp\parallel} I_3 + (b_{\perp\parallel} I_2 I_3 + c_{\perp\parallel} I_5) / R_{\perp\parallel} = R_{\perp\parallel}^2 \quad \dots \text{NF}_{\perp\parallel}$$

$$F_{\perp}^{\tau}: a_{\perp}^{\tau} I_2 + b_{\perp}^{\tau} I_4 / R_{\perp}^c + c_{\perp}^{\tau} I_3 R_{\perp}^c / R_{\perp\parallel}^2 = R_{\perp}^c \quad \dots \text{SF}_{\perp}$$

- Crushing - (porous matrix) -

$$F_{\perp}^{cr}: a_{\perp}^{cr}I_2 + b_{\perp}^{cr}I_4 = R_{\perp}^{cr} \dots CrF_{\perp}$$

The prediction of failure - made by whichever condition - is satisfied first. Terms in table 3 enveloped by dots are *local correction* terms to approximate (fit) the mixed fracture domains. They are not *global interaction* terms as e.g. in the global fracture criteria of Tsai-Wu.

The stresses  $\tau_{21}$  and  $\sigma_1^t$  do not have a common action plane, but marginally act micromechanically together. However,  $\tau_{21}$  and  $\sigma_1^c$  almost have the same action plane in case of brittle constituents fibre and matrix.

How the stress efforts are adding, linearly or quadratically or even cubically is determined by the course of test data.

The fracture type Crushing Fracture is added in Table 3 for reasons of completeness. It belongs to a material which due to its porosity will fail by internal *voluminous* degradation under compressive stresses and not in "planes" any more.

### 4.3 Determination of IFF Calibration Conditions besides the Basic Strengths

- Putting the compressive strength  $R_{\perp}^c$  into  $F_{\perp}^{\tau}$  delivers  $a_{\perp}^{\tau} = b_{\perp}^{\tau} - 1$ . (4.1)

A second equation, if using the measurable fracture angle  $\Theta_{fp}^c$  as the other obtainable information of the lateral compression test will be Mohr-Coulomb's condition ( $\hat{c} = \cos \theta_{fp}^c$ )

$$-\frac{\partial F_{\perp}^{\tau}}{\partial \sigma_n} / \frac{\partial F_{\perp}^{\tau}}{\partial \tau_n} = -\mu_{\perp\perp} = +\cot \alpha_n \ 2\Theta_{fp}^c = 0,5 \left( \frac{\hat{c}}{\hat{s}} - \frac{\hat{s}}{\hat{c}} \right) \text{ yielding } b_{\perp}^{\tau} = 1/(4\hat{c}^2 - 1). \quad (4.2)$$

- Trials to estimate the tensile fracture stress  $\sigma_{\perp}^{tt}$  in an appropriate test had no success [VDI97]. However, a good estimation can be achieved by using the information  $R_{\perp}^c$  being Weibull distributed. Following [Awa78] easily can be derived

$$\sigma_{\perp}^{tt} = R_{\perp}^t / \sqrt[k]{2} \quad \text{with } k = \text{Weibull's module.} \quad (4.3)$$

- With respect to Fig. 6 a value for a point on the "bulge" ( $\tau_{\perp\parallel}^{2D}, \sigma_{\perp}^{2D}$ ) can be estimated or directly a value for the linearized slope  $m_{\perp\parallel} \approx (\tau_{\perp\parallel}^{2D} - R_{\perp\parallel}) / \sigma_{\perp}^{2D}$  (4.4)

### 4.4 Analytical Derivation of Mohr's Envelope Curve

Resolving the fracture condition  $F_{\perp}^{\tau} = 1$  for  $\sigma_2$  delivers in case of  $\tau_{23} = 0$

$$\sigma_2 \cdot 2b_{\perp}^{\tau} = -R_{\perp}^c a_{\perp}^{\tau} + 2\sigma_3 b_{\perp}^{\tau} + \sqrt{a_{\perp}^{\tau 2} R_{\perp}^{c2} - 8a_{\perp}^{\tau} R_{\perp}^c b_{\perp}^{\tau} \sigma_3 + 4b_{\perp}^{\tau} R_{\perp}^{c2}} = f(\sigma_3) \quad (4.5)$$

$$\text{with } \tilde{c} = \sqrt{(a_{\perp}^{\tau} R_{\perp}^c - 2b_{\perp}^{\tau} \sigma_3 + 2b_{\perp}^{\tau} \sigma_2) / (4b_{\perp}^c / (\sigma_2 - \sigma_3))}, \sigma_3 = \text{variable} \quad (4.6)$$

$$\text{and } \tau_{nt} = | \tilde{s} \tilde{c} (-\sigma_2 + \sigma_3) |, \sigma_n = \tilde{c}^2 \sigma_2 + \tilde{s}^2 \sigma_3, \tilde{s} = \sqrt{1 - \tilde{c}^2}. \quad (4.7)$$

Then the cohesion can be calculated from  $R_{\perp}^{\tau} = \tau_{nt} (\sigma_n = 0)$ . This quantity corresponds to Puck's  $R_{\perp\perp}^A$  [Puc96].

## 5 PROBABILISTIC MODELLING OF MULTIPLE FAILURE DOMAINS

The application of probabilistics will connect adjacent modes.

The influence of the FF modes on IFF can be taken into account very simply by practical correction terms (see [Cun96/1]) in the IFF conditions *or* by probabilistics as shown now.

To estimate the *joint probability of failure* of the different IFF modes as *logical model of the failure system* the series system or union U of  $\ell = 3$  IFF failures will be taken. This delivers a failure probability  $p_f$  on the safe side (index S for sum, see [Cun96/2]), of

$$p_f \leq \sum p_{f,\ell} = 1 - (1-f_{\perp}^{\sigma S})(1-f_{\perp\parallel}^S)(1-f_{\perp}^{\tau S}) \quad (5.1)$$

since small  $p_{f,\ell}$  are expected. Correlation among the  $\ell$  (component) failures leads to a smaller (system) failure probability  $p_f$ , above expression therefore is conservative. In case of a Weibull-distributed strengths  $R_{\perp}^t, R_{\perp}^c, R_{\perp\parallel}$  as "sum" function

$$f^S = 1 - \exp\left[-\left(\frac{r}{w}\right)^k\right] \quad (5.2)$$

is valid (it represents the distribution of the extreme defects) with  $r$  = stress variable,  $k$  = Weibull's module (characterising the scatter of a strength) and  $w$  = shape parameter. A further parameter  $\tau$  characterising the position of the distribution is put zero. This is in any case permitted for very brittle materials (e.g. monolithic ceramics,  $k \geq 2$ ). An estimation of Weibull's parameter is possible [Pli95] on basis of the mean value  $m$  and the coefficient of variation of the parent distribution of each strength measured (bounds:  $cov < 25\%$ ,  $k > 4,8$ ) by

$$k \approx 1.2 / cov; \quad w = m / \Gamma(1+1/k); \quad m = \bar{R} \quad \text{with} \quad \Gamma = \text{Gamma function.} \quad (5.3)$$

As estimations for  $m$ ,  $v$  the values of a well sized sample are taken *without* considering the confidence interval.

Combining (5.1) and (5.2) yields the following equation for the IFF body

$$\left(\frac{r_{\perp}^{\sigma}}{w_{\perp}^{\sigma}}\right)^{k_{\perp}^{\sigma}} + \left(\frac{r_{\perp\parallel}}{w_{\perp\parallel}}\right)^{k_{\perp\parallel}} + \left(\frac{r_{\perp}^{\tau}}{w_{\perp}^{\tau}}\right)^{k_{\perp}^{\tau}} = -\ell_n(1-p_f). \quad (5.4)$$

Instead of a uniaxial stress the *equivalent stress* as representation of the multiaxial state of stress will be put in (5.4):  $r_{\perp}^{\sigma} = \sigma_{\perp}^{\sigma}$ ,  $r_{\perp\parallel} = \sigma_{\perp\parallel}$ ,  $r_{\perp}^{\tau} = \sigma_{\perp}^{\tau}$ . It can be calculated in case of  $F_{\perp}^{\tau}$  (shorter than for the IFF cases having cubic invariants)

$$F_{\perp}^{\tau} = f_{Res_{\perp}}^{\tau} \sigma_{\perp}^{\tau} / R_{\perp}^c = 1 \quad \text{or} \quad \sigma_{\perp}^{\tau} = R_{\perp}^c / f_{Res_{\perp}}^{\tau} \quad (5.5)$$

$$f_{Res_{\perp}}^{\tau} = [-a_{\perp}^{\tau} I_2 + \sqrt{a_{\perp}^{\tau 2} I_2^2 + 4b_{\perp}^{\tau} I_4 + 4c_{\perp}^{\tau} R_{\perp}^c / R_{\perp\parallel}^2}] / 2[b_{\perp}^{\tau} I_4 / R_{\perp}^c + c_{\perp}^{\tau} I_3 R_{\perp}^c / R_{\perp\parallel}^2].$$

For the IFF Proof of Design an engineering approach estimates  $f_{Res}$  in the mixed failure domain

$$(1 / f_{Res})^k = (1 / f_{Res_{\perp}}^{\sigma})^k + (1 / f_{Res_{\perp\parallel}})^k + (1 / f_{Res_{\perp}}^{\tau})^k = f(f_{Res}^{(modes)}) \quad (5.6)$$

(MFD) with  $k \approx \min k$  (safe side) causing a maximum out-smoothing.

## 6 APPLICATION TO GLASS/EPOXIDE-FRP

### 6.1 Determination of Curve Parameters (applying MATHCAD)

For the application of the criteria achieved at first all informations on the basic strengths: The type of distribution, the mean value  $\bar{R}$  and the coefficient of variation  $cov$  have to be provided. Table 4 represents an example set of data. The sources are various investigations [Kna72], [ZTL], [VDI97], due to the fact that a real complete test series of all interesting combinations of stresses including  $\sigma_1$  for FRP is not existing.

Table 4: Strength Properties ( $v_f = 0.60$ ) and data of Calibration Points (mean values)

$\bar{R}_{\parallel}^t$ :	Weibull,	1500 MPa,	cov = 6 %
$\bar{R}_{\parallel}^c$ :	Weibull,	1200 MPa,	cov = 7 %
$\bar{R}_{\perp}^t$ :	Weibull,	40 MPa,	cov = 12 %
$\bar{R}_{\perp}^c$ :	Weibull,	144 MPa,	cov = 7 %
$\bar{R}_{\perp\parallel}$ :	Weibull,	61 MPa,	cov = 10 %



$$\bar{\theta}_{fp}^c = 49^\circ; \tau_{\perp}^{\tau} = 73 \text{ MPa}; \sigma_{\perp}^{\tau} = -95 \text{ MPa}$$

$$\sigma_{\perp}^{\text{tr}} = -86 \text{ MPa}, \tau_{\perp}^{\sigma} \approx 1.05 R_{\perp\parallel} (\sigma_2 = 0)$$

$$(\sigma_2, \tau_{21}) = (40, 0), (28, 40), (0, 58), (-90, 72)$$

## 6.2 Fracture Curves: Deterministic Approach incl. Effect of Correction Terms

Fig. 4 comprises four different cross-sections of the five-dimensional IFF-body ( $\sigma_2, \sigma_3, \tau_{23}, \tau_{31}, \tau_{21}$ ): The graph ( $\tau_{21}, \sigma_2$ ) represents stresses in the plane of the lamina which are of highest interest in the justification of the stress-output delivered from Classical Laminate Theory (CLT). Three curves  $F_{\perp\parallel}^{\tau}$  (transversal SF),  $F_{\perp\parallel}$  (transversal-parallel SF) and  $F_{\perp\parallel}^{\sigma}$  (transversal-parallel NF) envelope the "50 % safe domain". The graph ( $\tau_{31}, \sigma_2$ ) outlines by "Puck's corner" that in contrary to ( $\tau_{21}, \sigma_2^t$ ) the shear stress  $\tau_{31}$  has *not* the same action plane as  $\sigma_2^t$ . The remaining two graphs ( $\sigma_2, \sigma_3$ ) and ( $\tau_{23}, \sigma_2$ ) are well-known from isotropic materials. In these isotropic cross-sections fracture can be described excellently by the homogenised lamina stresses ( $\sigma_2, \sigma_3, \tau_{23}$ ) or artificially smeared stresses, respectively. In the hydrostatic domain  $\sigma_2^c = \sigma_3^c \approx -10 R_{\perp}^c$  the IFF cureves will be closed by  $F_{\perp\parallel}^z$ , due to Poisson's effect.

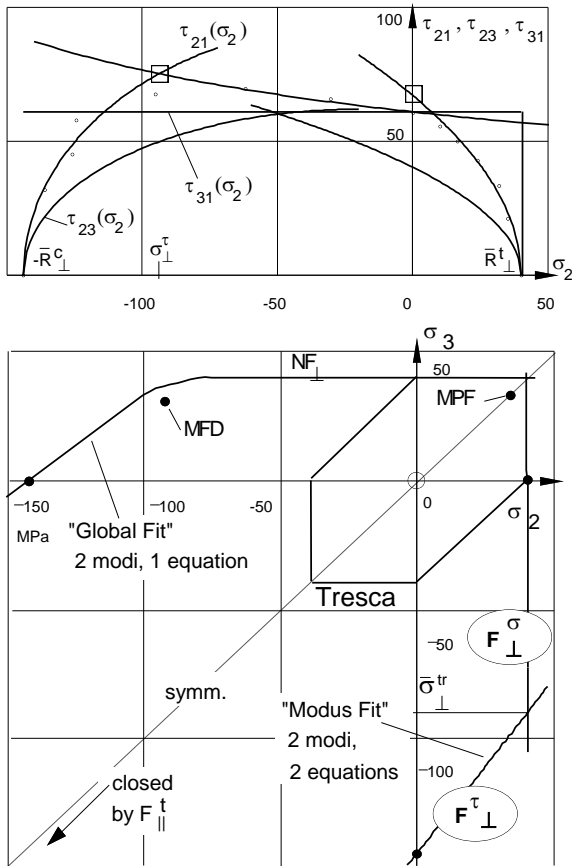


Fig. 4: IFF-curves (Glass FRP). (MFD = mixed failure domain = fracture due to 2 modes, MPF = multiplane fracture of the same mode NF  $\perp$ )

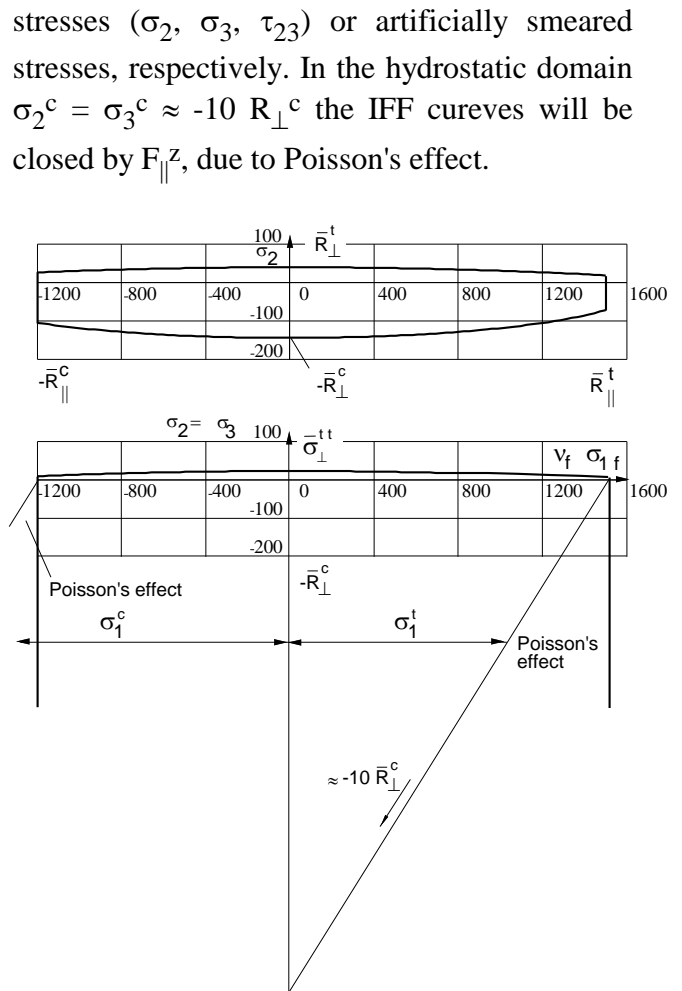


Fig. 5: FF- and IFF-curves (Glass FRP). (with correction terms, different scales)

Fig. 5 outlines the limited applicability of the homogenized lamina stresses. The lamina (composite) stress  $\sigma_1$  is not the fracture active stress, however, the stress  $\sigma_{1f}$  of the constituent (material) fibre. In order to nevertheless remain in the graphical display on composite level the

fibre stress has to be multiplied by the fibre volume fraction  $v_f$ . This should be an acceptable approach due to the extreme difference in the stiffness and thereby in the load carrying capacity of fibre and matrix. Tests performed, see [VDI97], show the effect of Poisson: Under biaxial compression the load can be only increased until tensile fracture stress or strain of the fibre will be met.

### 6.3 Simple 2D-Approximation of the $(\sigma_2, \tau_{21})$ Fracture Curve

For an improved but nevertheless simple approximation of the  $(\sigma_2, \tau_{21})$ -test results, which are mandatory for the evaluation of CLT stresses, the utilisation of the formulae

$$F_{\perp\parallel}^{\sigma}: a_{\perp}^{\sigma} \sigma_2 / R_{\perp}^t + c_{\perp}^{\sigma} \sigma_2^2 / R_{\perp}^{t2} + d_{\perp}^{\sigma} \tau_{21}^2 / R_{\perp\parallel}^2 + e_{\perp}^{\sigma} \sigma_2 \tau_{21}^2 / R_{\perp\parallel}^3 = 1 \quad (6.1a)$$

$$F_{\perp}^{\tau}: a_{\perp}^{\tau} \sigma_2 / R_{\perp}^c + b_{\perp}^{\tau} \sigma_2^2 / R_{\perp}^{c2} + c_{\perp}^{\tau} \tau_{21}^2 / R_{\perp\parallel}^2 = 1 \quad (6.1b)$$

is recommended with  $a_{\perp}^{\tau}, b_{\perp}^{\tau}$  from the equations (4.1, 4.2) and the calibration points indicated in Fig. 6 by a square. Due to micromechanical interaction caused by the matrix the author micromechanically combines  $NF_{\perp\parallel}$  and  $NF_{\perp}$  in his approach (Puck:  $SF_{\perp}$  and  $SF_{\perp\parallel}$  macromechanically).

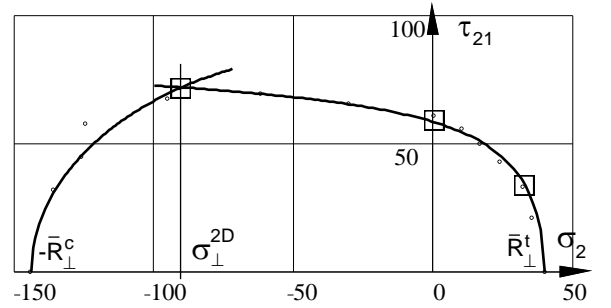


Fig. 6: 2D-Approximation (50%, Mean Curve).  $\circ$  Test Data from [Kna72].  $\square$  calibration points

### 6.4 Fracture Curves: Probabilistic Approach

The probabilistic out-smoothing in the MFD or transition zone, resp., of the piecewise smooth fracture-type related domains of the IFF-body shall be visualised by Fig. 7.

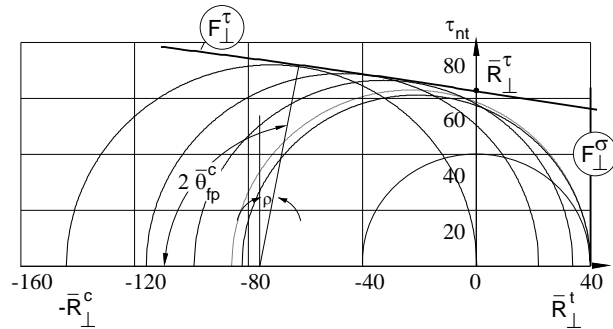


Fig. 8: An analytically derived Mohr-Coulomb "Envelope" Curve (bold) with MFD-circles and Transition Circle (dashed).

( $R_{\perp}^{\tau} = \text{friction cohesion}, \rho = \tan \mu_{\perp\perp}$ ,

$$\mu_{\perp\perp}^c = -\cot \text{an } 2\theta_{fp}^c)$$

Further the traditional "global fit" by polynomial interaction failure models (applied by most of the traditional strength criteria) is compared with the "modus fit" proposed in this article. The application of the probabilistic out-smoothing leads again back to one equation for the description of the global course of test data. Based on the numerical investigations for Fig. 7 one further conclusion can be drawn that

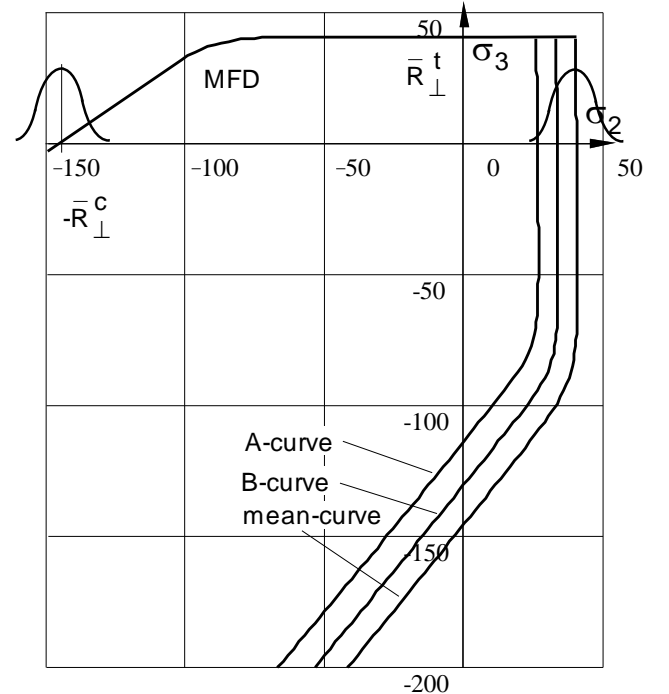


Fig. 7: "Global Fit" versus "Modus Fit". Design curves showing Probabilistic Out-smoothing in the Mixed Failure Domain (MFD)

multiple fracture in a mode, e.g.  $NF_{\perp}$  caused by biaxial tensile stresses, will be not covered by the simple modulus fit ( $c_{\perp}^{\sigma} = 0$ ). This correction term is necessary to approximate the test data in the MPF regime. Beside this, the term also has an effect in the MFD regime ( $SF_{\perp}$ ,  $NF_{\perp}$ ), which is not adverse because such brittle materials with a high contents of defects show both sorts of out-smoothing.

Essential for the dimensioning of FRP-structures is the "B-value Design Curve", most often.

Fig. 8 eventually shows (probably for the first time) an analytically derived Envelope Curve. To remind us of the former enveloping procedure the compression circle and the transition (the fracture mechanism jumps from  $NF_{\perp}$  to  $SF_{\perp}$ ) circle are included. Also the relationship of fracture angle, friction angle  $\rho$  and the local Coulomb friction coefficient  $\mu_{\perp\perp}^c$  derived from a  $R_{\perp}^c$ -loading are given.

In the MFD no realistic fracture angle will be determined. Consequently the  $\tau_{nt}(\sigma_n)$  curve again has to be an envelope of the circles ( $\sigma_2^d, \sigma_3$ ) or ( $\sigma_2, \sigma_3^d$ ) the values of which are the curve points of the probabilistic function (5.4) describing the transition from  $SF_{\perp}$  to  $NF_{\perp}$ .

And, looking at the FEM codes the fracture conditions offered for a so-called "linear or parabolic Mohr-Coulomb Material" is nothing but a continuous mathematical description of an envelop of Mohr's circles in the MFD. It just has relation to Mohr's fracture angle outside the MFD where a "pure"  $SF_{\perp}$  or  $NF_{\perp}$  mode is dominating.

## CONCLUSIONS, OUTLOOK AND REMARKS

### Test Data Fit and Failure Modes:

- The author has the same point of view as L.J. Hart-Smith: It is scientifically incorrect to employ polynomial interaction failure models whenever the (micromechanical) failure mechanism of the critical constituent of the composite changes with the state of stress. And - valid for any material - the main shortcoming of global criteria is: A change in one strength (which belongs to a distinct fracture mode) has an effect on the *whole failure surface (surface of fracture body)* which represents all modes ([Har93, Cun94]). Interactions between *different* failure modes are incorrect. Interactions between stresses affecting the *same* failure mode in the *same* constituent of the composite are permitted.
- Separate characterisations are needed for *each* failure mechanism in *each* constituent of a composite of materials. The fit has to be performed for each mode separately.
- It does not matter whether a state of stress comes from a one-, a two- or a three-dimensional stressing as long it belongs to one fracture mechanism or mode. Consequently all these states of stress can be described by the *same* fracture condition.
- In the isotropic planes test data excellently can be described by the homogenized stresses  $\sigma_2, \sigma_3, \tau_{23}$  (composite = smeared or averaged material). However, if the UD-lamina is e.g. subjected to  $(\sigma_1, \sigma^2, \sigma^3)$  the constituent (real isotropic or anisotropic material) stress  $\sigma_{1f}$  will be responsible for fracture and not the composite stress ( $\sigma_1$ ).

### Strength Criteria:

- There are 3 categories of failure criteria: stress-based, strain-based and energy-based. The criteria can be grouped into independent, partly (stress) interactive and globally interactive ones. Their development may be based on micromechanical (constituent level) and/or (meso/) macromechanical investigations (lamina resp. composite level).

- The author prefers stress criteria in the proof of design because: stresses fracture the material, residual stresses are taken into account and strain history is considered in the strength values.
- The concept of strength criteria presented exhibit a physical basis, a good fit of test data course, invariance with respect to coordinate transformations, a relatively easy application involving numerical stability and applicability to ductile behaving composites as well.
- From the several applications a preliminary assessment of the concept is possible:
  - the fracture conditions  $F = 1$  determine the shape of the failure surface with its five piece-wise smooth areas, representing the five modes
  - a separation of mechanical and probabilistic modelling would be advantageous for an accurate interpretation of test results but is not completely possible. The probabilistic tool has to be taken to smooth-out in the mixed failure domain (MFD) resp. transition domain of two or more modes the adjacent mode-related pieces of the "failure surface"
  - the out-smoothing approximately can be done by applying correction terms instead of performing real probabilistic calculations
- The application of the concept to various isotropic test results was very successful and is very promising in case of transversally-isotropic UD-laminae, too. A big challenge will be an application to the various woven fabric laminae.
- Because "high tech" composite parts normally have notches and often have to be designed to damage tolerance they were qualified more or less by tests. So, the physical drawbacks of the traditional strength criteria applied to unnotched (and notched) structures have not been revealed.

### **Design (dimensioning) and Proof of Design:**

- There are 5 basic strengths (or 5 resistances, if Mohr would be strictly applied) and as much modes or fracture mechanisms, respectively.
- To establish 3D-design curves the concept just needs for the "fitting" of the 5 pure modes the 5 basic strength allowables, the fracture angle  $\theta_{fp}^c$  (pertaining Coulomb's friction) and a calibration point at the  $(\sigma_2, \tau_{21})$ -bulge. If micromechanical interaction will be taken into account 3 more calibration points have to be provided or can be assumed from experience with a FRP family in order to determine the remaining curve parameters belonging to the correction terms. The curve parameters of each failure function in this paper are computed- beside the basic strength points - from further distinct calibration points, only. Generally of course, a root mean square-fit is foreseen to achieve their values.
- For the dimensioning the designer needs the coloured contour plots or profiles of the stresses as output of the FEM stress analysis and for the Proof of Design he should get offered by the FEM codes coloured profiles of  $f_{Res}^{mode}$  too. This is indirectly still practiced when plotting the equivalent stress of v. Mises ( $3 J_2 / \sigma_{yield}^2 = 1 \rightarrow f_{Res}^{mode} = (\sigma_{yield}^2 / \sigma_{equiv}^2)^{0,5} = \sigma_{yield}^2 / 3J_2)^{0,5}$ ) plots for the mode "onset of yielding" in case of isotropic material or for NF with the principal tensile stress ( $\sigma_I / R^t = 1 \rightarrow f_{Res}^{mode} = R^t / \sigma_I$ ). The lowest  $f_{Res}^{mode}$  computed for IFF and FF drives the design.
- In the mixed failure domain equ. (5.6) delivers an estimation for  $f_{Res} = f(f_{Res}(modes))$ , therewith bypassing together with the correction terms a real probabilistic out-smoothing.
- The determination of  $f_{Res}$  in case of cubic invariants is a little more laborious. If residual stresses have to be taken into account, due of  $f_{Res} \cdot \{\sigma\}^{(load)} + \{\sigma\}^{(residual)}$ , see [VDI97].

## Acknowledgements:

The author highly appreciates the excellent support of his colleague B. Szelinski, the fruitful discussions with Dr. "John" Hart-Smith and the comments of members co-operating under the German R&D contract number 03N8002 of the BMBF [VDI97].

## REFERENCES

- [Awa78] Awaji, H. and Sato, S.: A Statistical Theory for the Fracture of Brittle Solids under Multiaxial Stresses. *International Journal of Fracture* 14 (1978), R13-16
- [Boe85] *Boehler, J.P.*: Failure criteria for glass-fiber reinforced composites under confining pressure. *J. Struct. Mechanics* 13, 371-393
- [Cun96/1] *Cuntze, R.G.*: "Fracture-type Strength Criteria" formulated by Invariants which consider the Materials Symmetries of the Isotropic/Anisotropic Material used. Conf. on Spacecraft Structures, Materials and Mechanical Testing. ESA-CNES-DARA: Noordwijk, March 1996
- [Cun96/2] *Cuntze, R.G.*: Bruchtypbezogene Auswertung mehrachsiger Bruchtestdaten und Anwendung im Festigkeitsnachweis sowie daraus ableitbare Schwingfestigkeits- und Bruchmechanikaspekte. DGLR-Jahrestagung, Dresden, Sept. 96, Tagungsband 3
- [Fla82] *Flaggs, D.L., Kural, M.H.*: "Experimental Determination of the In Situ Transverse Lamina Strength in Graphite Epoxy Laminates". *J. Comp. Mat.* Vol 16 (1982), S. 103-116
- [Har93b] *Hart-Smith, L.J.*: An Inherent Fallacy in Composite Interaction Failure Curves. *Designers Corner, Composites* 24 (1993), 523-524
- [Has80] *Hashin, Z.*: Failure Criteria for Unidirectional Fibre Composites. *J. of Appl. Mech.* 47 (1980), 329-334
- [Huf95] *Hufenbach, W. and Kroll, L.*: A New Failure Criterion Based on the Mechanics of 3-Dimensional Composite Materials. ICCM-10, Whistler, Canada, 1995
- [Jel96] *Jeltsch-Fricker, R.*: Bruchbedingungen vom Mohrschen Typ für transversal-isotrope Werkstoffe am Beispiel der Faser-Kunststoff-Verbunde. *ZAMM* 76 (1996), 505-520
- [Kna72] *Knappe, W. und Schneider, W.*: "Bruchkriterien für unidirektionalen Glasfaser/Kunststoff unter ebener Kurzzeit- und Langzeitbeanspruchung". *Kunststoffe*, Bd. 62 (1972), 864
- [Kop96] *Kopp J. and Michaeli, W.*: Dimensioning of Thick Laminates using New IFF Strength Criteria and some Experiments for their Verification. Proceedings "Conf. on Spacecraft Structures Materials and Mechanical Testing", ESA, 27-29 March 1996
- [Moh00] *Mohr, O.*: Welche Umstände bedingen die Elastizitätsgrenze und den Bruch eines Materials? *Civilingenieur* 44 (1900), 1524-1530, 1572-1577
- [Pau61] *Paul, B.*: A Modification of the Coulomb Mohr Theory of Fracture. *J. of Appl. Mech.* (1961), 259-268
- [Puc92] *Puck, A.*: Ein Bruchkriterium gibt die Richtung an. *Kunststoffe* 82 (1992), S. 607-610 (A failure criterion shows the Direction - Further Thoughts on the Design of Laminates - *Kunststoffe German Plastics* 82 (1992), 29-32)
- [Puc96] *Puck, A.*: Festigkeitsanalyse von Faser-Matrix-Laminaten. (Modelle für die Praxis). München: Carl Hanser Verlag, 1996
- [Row85] *Rowlands, R.E.*: Strength (Failure) Theories and their Experimental Correlation. In Sih, G.C. and Skudra, A.M.: editors, *Handbook of Composites*, Vol. III, chapter 2, Elsevier Science Publisher B.V., Madison, WI, U.S.A., 1985, 71-125

- [Säh93] *Sähn, S. und Göldner, H.*: Bruch- und Beurteilungskriterien in der Festigkeitslehre. Fachbuchverlag Leipzig-Köln, 2. Ausgabe, 1993
- [Tsa71] *Tsai, S.W. and Wu, E.M.*: A General Theory of Strength for Anisotropic Materials. Journal Comp. Mater, Vol. 5 (1971), 58-80
- [VDI97] *Cuntze, R.G., et.al.*: Neue Bruchkriterien und Festigkeitsnachweise für unidirektionalen Faserkunststoffverbund unter mehrachsiger Beanspruchung - Modellbildung und Experimente -. VDI-Fortschrittbericht, Reihe 5. BMBF-Vorhaben 03N8002 (A. Puck, adviser until 1995)
- [ZTL] Dornier, Fokker, MBB, DLR: Investigations of Fracture Criteria for Laminae (in German). 1975-1980, Grant from Ministry of Defence, BMVg, Koblenz

# EVALUATION OF MULTIAXIAL TEST DATA OF UD-LAMINAE BY SO-CALLED "FRACTURE-TYPE STRENGTH CRITERIA" AND BY SUPPORTING PROBABILISTIC MEANS

*Ralf G. Cuntze*

*Division of Spacecraft, MAN Technologie AG  
Liebigstr. 5a, 85757 Karlsfeld/Munich. Fax 0049-8131-89-1939  
(lecturer at Universität der Bundeswehr, München)*

**Keywords:** Fibre reinforced composites, strength criteria, test data evaluation

## OVERVIEW

Overall objective of this elaboration is to calibrate fracture criteria resp. to define size and shape of the fracture body as cheaply as possible by executing the characteristic tests only.

Based on knowledge, achieved by investigating *v. Mises, Mohr - Coulomb* and the new physically based *Hashin - Puck* Strength Criteria for inter fibre fracture (IFF) of brittle unidirectional laminae, a new and general concept for the derivation of fracture criteria will be proposed and applied to fibre reinforced plastics (FRP).

The fracture body derived here is basically piecewise smooth, each piece representing a single *failure mode*. As interpolation functions the *invariants* associated to the material's symmetries are utilised. Physical basis is the reference to the 2 fracture-types (Fig. 1) in a material: normal fracture (NF) and shear fracture (SF). For the subsets of failure modes "fibre fracture (FF)" and "IFF" two conditions for FF and three for IFF are derived. These five conditions describe the five failure mechanisms occurring, and five failure modes are the maximum number a transversally-isotropic material, modelled a crystal, can possess. There are also 5 strengths, only, and each strength governs one mode.

In the transition zone of two failure modes or domains of mixed fracture, respectively, a probabilistic modelling has to be applied. This finally will lead again to a smooth surface of the complete fracture body and smooth fracture curves (Fig. 2).

## RESULTS AND PRINCIPAL CONCLUSIONS

As one remarkable result of the elaboration has to be pointed out: Consider micromechanics resp. real material stresses in the constituents fibre and matrix (incl. interface) which only can fail, however, formulate and visualise in lamina stresses at composite resp. macromechanical level, and think in Mohr's fracture stresses.

The application of the criteria to test results is very promising (Fig. 3). Erroneous reserve factors, possible if applying the traditional global (stress) interaction criteria, should not be achieved.

To establish 3D-design curves the concept just needs for the "fitting" of the 5 pure modes the 5 basic strength allowables, the fracture angle  $\theta_{fp}^c$  under  $\sigma_2^c$  and a calibration point at the  $(\sigma_2, \tau_{21})$ -bulge. If micromechanical interaction will be taken into account 3 more calibration points have to be provided or can be assumed from experience with a FRP family in order to determine the remaining curve parameters.

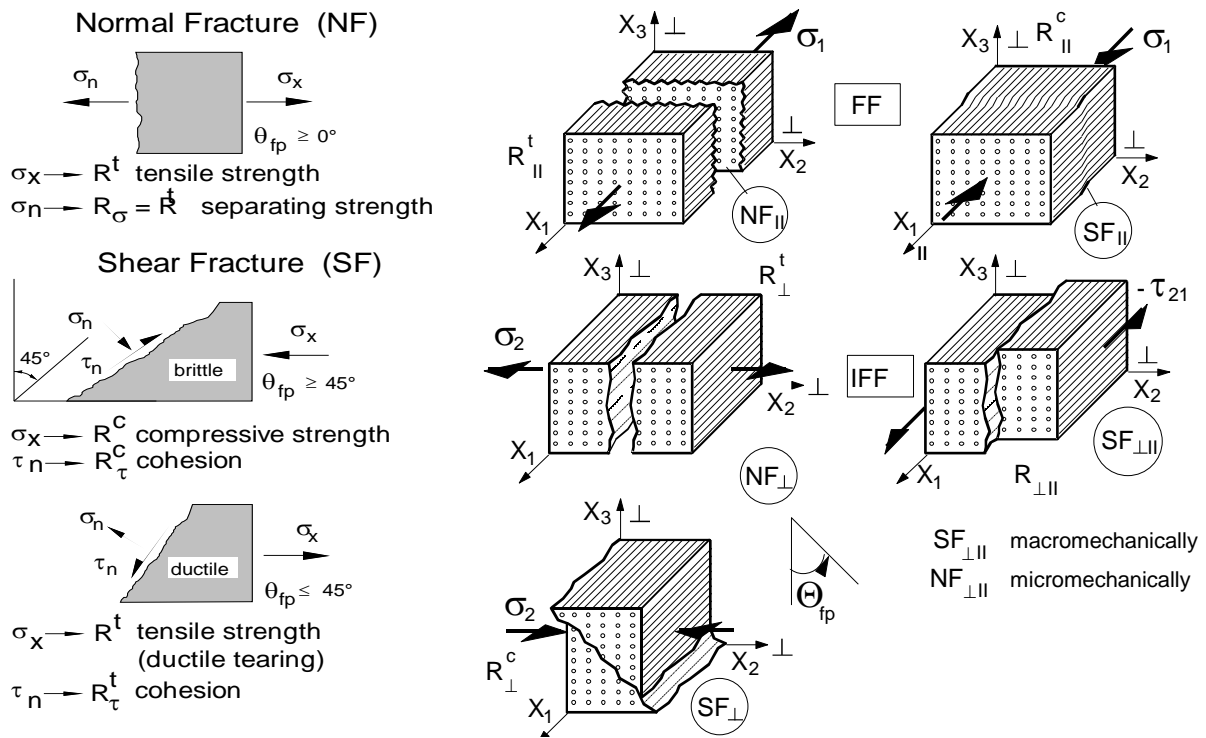


Fig. 1: Fracture Types ( $\equiv$  modes) in case of Brittle and Ductile behaving Isotropic Material and Fracture Modes in case of Transversally-isotropic Material ( $\sigma_n^A$  ( $\theta = \theta_{fp}$ ) =  $\sigma_n$ ).  
 (c: = compression, t: = tension,  $\{\sigma\} = (\sigma_1, \sigma_2, \sigma_3, \tau_{23}, \tau_{31}, \tau_{21})^T$ )

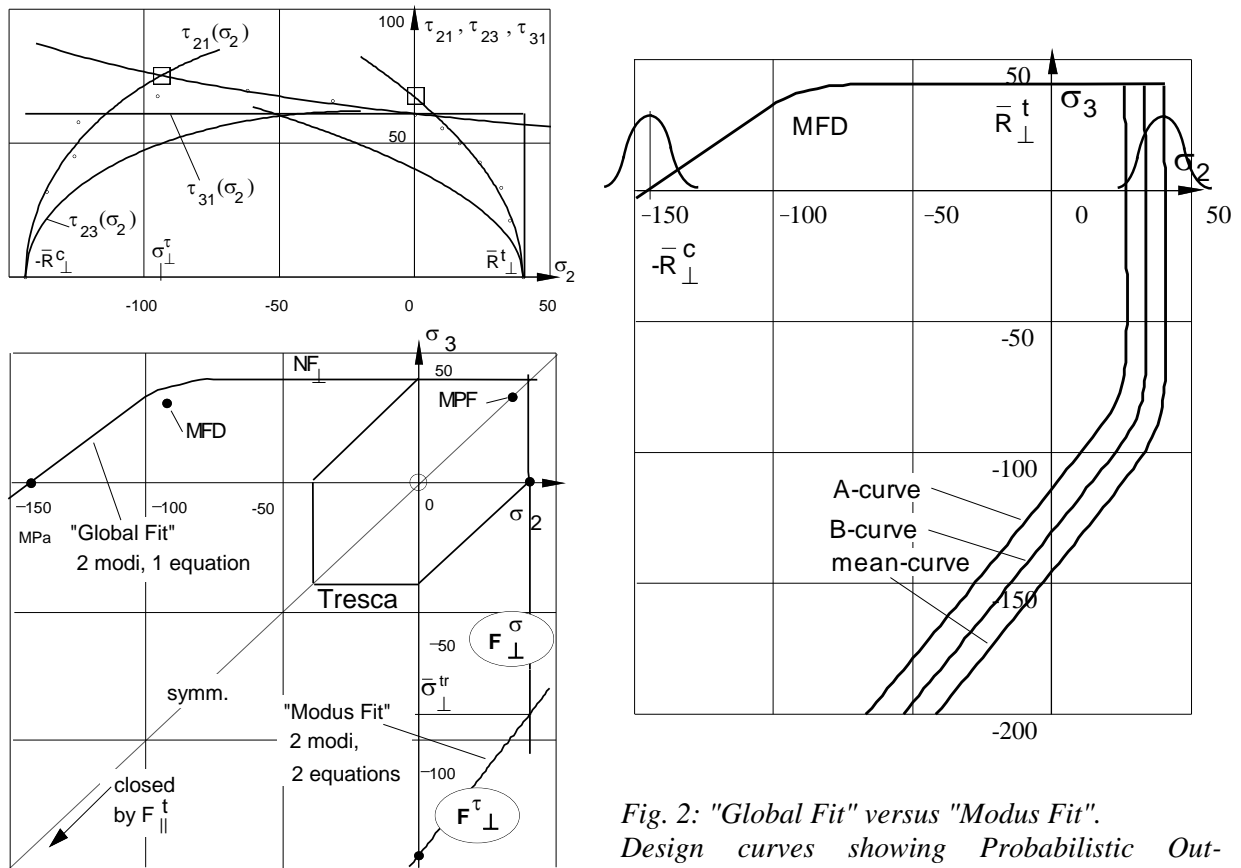


Fig. 3: IFF-curves (Glass FRP). (MFD = mixed failure domain = fracture due to 2 modes, MPF = multiplane fracture of the same mode NF<sub>⊥</sub>)

Fig. 2: "Global Fit" versus "Modus Fit". Design curves showing Probabilistic Out-smoothing in the Mixed Failure Domain (MFD) of the ( $\sigma_2, \sigma_3$ ) cross section of the fracture body